JOURNAL OF CIVIL ENGINEERING AND MANAGEMENT
ISSN 1392-3730/eISSN 1822-3605
2016 Volume 22(4): 470–479
doi:10.3846/13923730.2014.897992

NUMERICAL STUDIES ON SMOKE SPREAD IN THE CAVITY OF A DOUBLE-SKIN FAÇADE

Jie JI, Yi Fan LI, Wen Xi SHI, Jin Hua SUN

State Key Laboratory of Fire Science, University of Science and Technology of China, Hefei 230026, China

Received 13 May 2013; accepted 27 May 2013

Abstract. In this paper, influence of two key factors, fire room height and outer pane tilt angle, on smoke spread in the cavity of a double-skin façade (DSF) was studied numerically. The fire room was located adjacent to the DSF on the 2nd, 4th and 6th floors, respectively. The outer pane tilt angle varied at 80°, 90° and 100°. All cases were under two fire heat release rates of 1 MW and 5 MW. Results suggested that fire room height and outer pane tilt angle had significant effects on smoke spread in the cavity. For different fire room heights, there were two markedly different scenarios of smoke spread in the cavity between two vertical panes in a high-rise building. For outer pane tilt angle, the DSF with an inward tilted or vertical outer pane was dangerous for the upper floors due to hot smoke adhering to the upper inner pane. However, the turbulent vortex in the DSF with an outward tilted outer pane prevented hot smoke flowing out from the fire room.

Keywords: double-skin façade, smoke spread, fire room height, outer pane tilt angle, cavity, CFD.

Introduction

Glass curtain-walled buildings could provide good views, better environmental contributions and architectural aesthetics. They have been a fashionable decoration so far. The conventional single-skin glass façade has numerous problems, such as bad ventilation, glare, heat in summer and cold in winter, especially in buildings with a high glass skin. Therefore, the double-skin façade is a good choice in managing the interaction between the outdoors and the internal spaces. According to Chan *et al.* (2009), double-skin façade (DSF) can be defined as a building façade covering one or several floors with multiple glazed panes. A DSF system is composed of an outer skin, an intermediate air cavity and an inner skin (Ding *et al*. 2005; Kim, Song 2007). The intermediate air cavity between the inner and outer skins extends through several floors, in which the air can be ventilated naturally or mechanically.

Previous studies on the DSF mainly focused on ventilation, thermal behaviors, daylighting, energy performance and so on (Gratia, De Herde 2004a, 2004b, 2004c, 2007a, 2007b; Hien *et al*. 2005). Results show that the DSF system is a more advantageous architectural feature compared with single-skin façade. However, fire safety for the DSF should be dealt with more carefully. If a fire erupts next to a DSF, the adjacent inner glass pane might be broken in exposing to the thermal radiation of burning. The hot smoke then will be ejected into the cavity due to the horizontal momentum of the ceiling jet. The air cavity is likely to become the channel for spreading the hot smoke, which will speed up the development of fire vertically. Chow *et al.* (2006, 2007) studied the smoke spreading in the cavity of DSF and discussed the effects of cavity depth on fire spreading in a physical scale model. Chow (2011) examined air flow driven out of a flashover room fire to the cavity of a DSF by the Fire Dynamic Simulator and suggested that wider air cavity depth would be more dangerous. Ding and Hasemi (2006) investigated the possibility of using natural ventilation system for smoke control in a DSF. Ni *et al.* (2007) discussed the influence of DSF on the potential of vertical fire spread experimentally, concluding the flame propagation process and smoke moving characteristics in the air cavity.

For a DSF system, the cavity depth, namely the distance between the inner and outer panes, usually can range from 800 mm to 2000 mm (Wigginton 1996; He, Mu 2003; Guo *et al.* 2004). Many practices have proved that this cavity depth range can give a better environmental performance by inducing air flow naturally or mechanically. In addition, the DSF with a tilted outer glass pane is usually required for a better architectural aesthetic (Chen 2010). Generally, the outer pane tilt angle of a DSF can range from 75° to 115° (inward tilt angle is 75°~90°, and outward tilt angle is 90°~115°) (Chen 2010). If a fire occurred in a room adjacent to a DSF,

Corresponding author: Jie Ji
E-mail: *jijie232@ustc.edu.cn*

Taylor & Francis
Taylor & Francis Group

the cavity depth and the outer pane tilt angle will have significant effects on smoke spread in the cavity. For a high-rise building, the fire room height also is a key factor. Almost previous studies about the smoke spread in the cavity of a DSF focused on the effect of the cavity depth, but little attentions had been focused on these factors, the fire room height and the outer pane tilt angle. Therefore, to investigate the influence of fire room height and outer pane tilt angle on the smoke movement in the DSF, a series of simulations was conducted in this paper, which could provide useful data for engineers to understand smoke movement mechanisms and design fire protection codes in DSF.

1. Simulation solver

Currently, for fire researchers, Computational Fluid Dynamics (CFD) (Chow 1996; Guo *et al.* 2009; Zhang *et al.* 2010) modeling is an effective approach to predicting various aspects of thermal fluid phenomena associated with fires. Fire Dynamic Simulator (FDS) (McGrattan *et al.* 2009a), developed by National Institute of Standards and Technology (NIST), is a CFD model of fire-driven fluid flow. The model has been subjected to numerous validations, calibrations and studies on the temperature and velocity fields in fires. For example, Ni *et al.* (2008) successfully predicted the fire properties of DSF with FDS. FDS solves numerically a form of the Navier-Stokes equations for thermally-driven flow. A description of the model, many validation examples, and a bibliography of related papers and reports may be found on http://www.fire.nist.gov/fds/.

It includes both DNS (Direct Numerical Simulation) model and LES (Large Eddy Simulation) model. The LES model, which is widely used in study of fire-induced smoke flow behavior, is selected in this study.

The Sub-Grid-Model (SGM) commonly used in LES is developed originally by Smagorinsky (Smagorinsky 1963). The eddy viscosity is obtained by assuming that the small scales are in equilibrium, by balancing the energy production and dissipation. The turbulent viscosity defined in FDS is (McGrattan *et al.* 2009b):

$$\mu_{LES} = \rho(C_S\Delta)^2[\frac{1}{2}(\nabla u + \nabla u^T)(\nabla u + \nabla u^T) - \frac{2}{3}(\nabla u)^2]^{\frac{1}{2}}, \quad (1)$$

where: C_s is an empirical constant and Δ is a length on the order of the size of a grid cell. The constant C_s in LES simulation is flow dependent and has been optimized over a range from 0.1 to 0.25 for various flow fields.

FDS has been subjected to many verification studies and improved since its first release in 2000. According to these validation studies, the constants, C_s, Pr_t and Sc_t, are set as default values in FDS for current paper as 0.2, 0.2 and 0.5, respectively.

Therefore, this paper adopted FDS5.5.3 to study the smoke spread in the cavity of a DSF.

2. Physical model setup

To discuss the effects of fire room height on the smoke spread in cavity, a seven-level building height of 21 m was selected as the model DSF1 illustrated in Figure 1. The fire room with dimensions of 8×8×3 m was located adjacent to the DSF on the 2nd, 4th or 6th floor. The cavity depth varied at 0.8 m, 1.4 m and 2.0 m. The fire source was located on the left side of room, which was 8 m from the inner glass pane as shown in Figure 2. The fire size was 1×1 m from the ground of 1 m. The fire heat release rate (HRR) of 5 MW (Chow 2009, 2011) was designed to represent one fully-developed room fire in previous studies. Considering the early fire, two HRRs of 1 MW and 5 MW with constant heat flux per unit area were used as the design fire. Since this paper focused on studying the smoke spread in the cavity of DSF, an opening width of 8 m and height of 3 m was given on the inner pane next to the fire room. As shown in Figure 2, the temperatures of hot gases in cavity were measured by 30 thermocouples. On the left side, a bunch of 15 thermocouples at a 1.5 m vertical interval was arranged 5 cm away from the inner pane to measure the air temperature next to the inner panes, similarly, on the right side, a bunch of 15 thermocouples was arranged to measure the air temperature next to the outer panes.

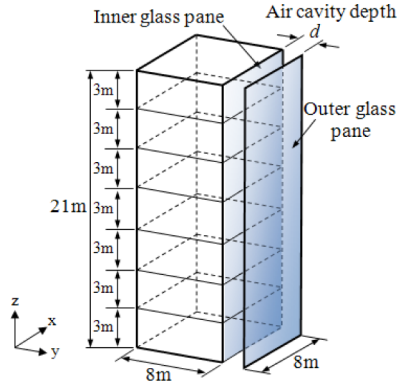

Fig. 1. Schematic diagram of physical model for DSF 1

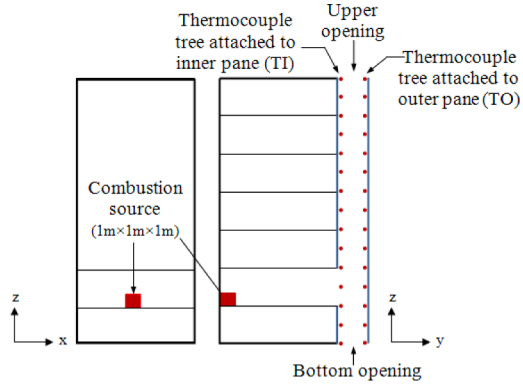

Fig. 2. Positions of thermocouples and the set of combustion source in DSF 1

In a DSF system with a tilted outer glass pane, the distance between inner and outer glass panes is small at one end of the air cavity, but relatively large at the other end. If a tilted DSF system extends through the whole high-rise building, there will be large waste of space due to the large distance between inner and outer glass panes at one end of the air cavity. Therefore, a DSF with a tilted outer glass pane is not very high and there may be two kinds of cases: (1) the tilted DSF system extends through the whole building height, but there are fewer floors in the whole building; (2) the tilted DSF system extends through several floors of a high-rise building.

A four-level model DSF2 of height 12 m was selected for studying the effects of outer pane tilt angle. The fire room was located on the 1st floor, with width of 8 m, depth of 8 m and height of 3 m. Six cases with an average cavity depth of 1.5 m were simulated, and the outer pane tilt angle θ varied at 80°, 90° and 100°, as shown in Figure 3.

All the boundary and initial conditions in all simulations were listed in Table 1.

3. Mesh sensitivity analysis

The sensitivity analysis of mesh grid size directly involves the result error of the computation, and even determines whether the result of calculation is plausible (Wang *et al.* 2005; Zhu *et al.* 2008).

Firstly, according to the physical model, we built a FDS model using a relatively coarse mesh, and then gradually refined the mesh. Comparing the results from a series of cases with different grid sizes, the calculation result which was independent of the mesh density could be found.

A measure (McGrattan *et al.* 2009b) of how well the flow field is resolved is given by the non-dimensional expression D^*/δ_x. δ_x is the nominal size of a mesh cell and D^* is a characteristic fire diameter. The calculating formula for D^* is:

$$D^* = \left(\frac{\dot{Q}}{\rho_\infty c_p T_\infty \sqrt{g}} \right)^{\frac{2}{5}}, \qquad (2)$$

where: $\dot{Q}$ is HRR, kW, ρ_∞ is ambient density, kg/m^3, c_p is specific heat capacity, kJ/(kg·K), T_∞ is ambient temperature,

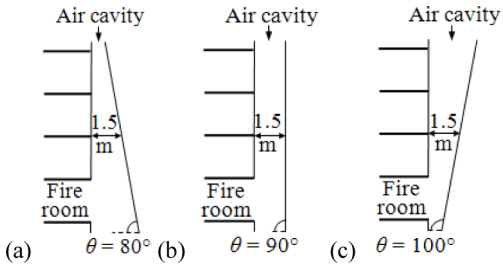

Fig. 3. Structure schematic diagram when (a) θ = 80°, (b) θ = 90° and (c) θ = 100° in DSF 2

Table 1. Condition of numerical simulations

Case No.		HRR (MW)	Total floors	Fire floor	d (m)	θ (°)
DSF1	A1	1	7	2	0.8	90
	A2	1	7	2	1.4	90
	A3	1	7	2	2.0	90
	A4	5	7	2	0.8	90
	A5	5	7	2	1.4	90
	A6	5	7	2	2.0	90
	A7	1	7	4	0.8	90
	A8	1	7	4	1.4	90
	A9	1	7	4	2.0	90
	A10	5	7	4	0.8	90
	A11	5	7	4	1.4	90
	A12	5	7	4	2.0	90
	A13	1	7	6	0.8	90
	A14	1	7	6	1.4	90
	A15	1	7	6	2.0	90
	A16	5	7	6	0.8	90
	A17	5	7	6	1.4	90
	A18	5	7	6	2.0	90
DSF2	A19	1	4	1	1.5	80
	A20	1	4	1	1.5	90
	A21	1	4	1	1.5	100
	A22	5	4	1	1.5	80
	A23	5	4	1	1.5	90
	A24	5	4	1	1.5	100

K, and g is gravitational acceleration constant, m/s^2. Recommended by McGrattan (2009b), D^*/δ_x should range from 4 to 16. According to Eqn (2), the single grid size of the finer mesh was calculated to be between 0.06 m and 0.24 m for the 1 MW fire in DSF1.

Obviously, finer grid will better reflect the heat flow field in detail, but it is also time consuming. So we have to make a choice for an appropriate mesh grid size. For 1 MW fire in DSF1, seven different grid sizes ranging from 0.06 m to 0.25 m were simulated for comparison, as shown in Table 2. The computational domain was divided into two meshes named MESH01 and MESH02. MESH01 was 8 m ($x1$) × 8 m ($y1$) × 4 m ($z1$), and MESH02 was 8 m ($x2$) × 4 m ($y2$) × 24 m ($z2$).

Figure 4 presented the vertical temperature next to the inner pane with above seven different grid sizes in Table 2. Along with refining the mesh, the temperature curve trended to be uniform. Results of the cases No. B5, B6 and B7 got slightly differences, and there was no significant improvement but more time consuming when the mesh density increased up to 10 grids/m. Therefore, we chose a mesh with the grid size of 0.10 m (10 grids/m) for the 1 MW fire in DSF1.

Table 2. Computing details of FDS simulation for mesh sensitivity analysis

Case No.	Grid quantity		Grids /m	Total running time of CPU (h:min:s)
	MESH01 (x1 × y1 × z1)	MESH02 (x2 × y2 × z2)		
B1	32×32×16	32×16×96	4	0:22:03
B2	40×40×20	40×20×120	5	0:48:48
B3	48×48×24	48×24×144	6	1:43:12
B4	60×60×30	60×30×180	7.5	4:34:48
B5	80×80×40	80×40×240	10	12:58:02
B6	100×100×50	100×50×300	12.5	28:26:40
B7	128×128×64	128×64×384	16	75:05:11

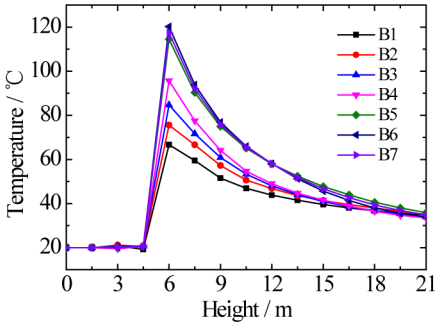

Fig. 4. Vertical temperature at the steady state next to the inner pane

4. Results and discussion

4.1. Effects of fire room height

Twenty four cases (from A1 to A24) were simulated in this section. With the cavity depth d of 1.4 m as an example, the smoke spread in the cavity is discussed in the following. Thermocouples, labeled as T_{in} and T_{out}, have been arranged as Figure 5.

When the fire was located on the 2nd, 4th and 6th floors respectively, the instantaneous temperature curves of T_{in} and T_{out} for d = 1.4 m were plotted in Figure 6. When the 1 MW fire was located on the 2nd floor as shown in Figure 6(a), T_{out} and T_{in} successively appeared maximum before 20 s, and then they decreased to 30 °C at the steady state. Oppositely, T_{in} and T_{out} were markedly different at the steady state when the fire was located on the 4th or 6th floor. In these two cases, T_{out} reached the maximum of 55 °C before 15 s, and then almost reduced to the outdoor temperature of 20 °C. After T_{out} appeared the maximum, T_{in} began to rise until a steady value of 75 °C averagely for a fire on the 4th floor and that of about 85 °C for a fire on the 6th floor. Due to the horizontal momentum of the ceiling jet, hot smoke ejected from the fire room and affected the outer glass pane firstly, resulting in the maximum of T_{out} before the rise of T_{in}. Then the smoke would be changed into vertical spreading from horizontal movement by the influence of heat buoyancy and differences in air entrainment above and below the hot window jet. The moving tendency of hot smoke in the cavity would influence the reliability of the inner and outer glass panes markedly. In view of Figure 6(a), it could be found that the gas temperatures next to the

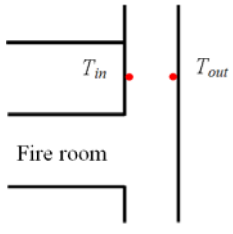

Fig. 5. Positions of T_{in} and T_{out}

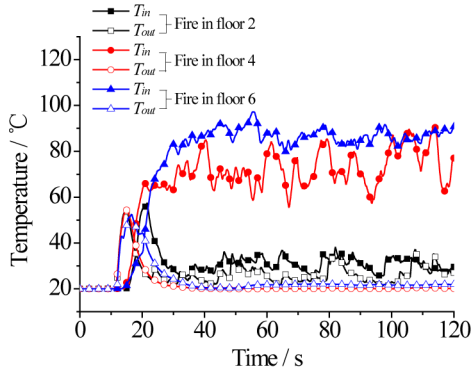

(a) Q = 1MW and d = 1.4m

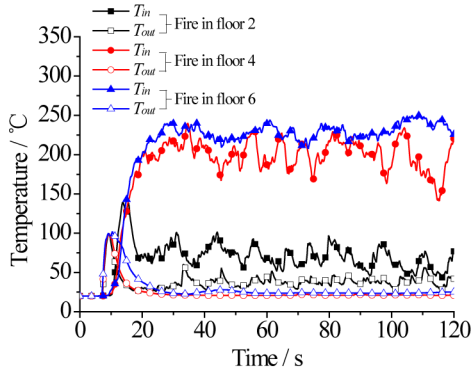

(b) Q = 5MW and d = 1.4m

Fig. 6. Instantaneous temperature curves of T_{in} and T_{out} with d = 1.4 m

inner and outer panes were markedly different for different fire room heights at the steady state. On the upper floor, the temperature difference between inner and outer panes was slight for a fire on the 2nd floor, but very obvious for the fires on the 4th and 6th floors. Due to the higher T_{in}, it was more dangerous for the upper inner glass pane when a fire was located on the 4th or 6th floor, especially on the 6th floor. When increasing the HRR to 5 MW as shown in Figure 6(b), the change tendency of curves was almost same with those in Figure 6(a).

With d = 1.4 m and Q = 5 MW, the temperature distributions at the steady state for the fires on the 2nd, 4th and 6th floors were shown in Figure 7. The following results could be observed from these temperature distributions.

(a) Fire on the 2nd floor:

In the process of spreading upwards within the cavity, smoke filled the upper cavity, resulting in that T_{in} and T_{out} were approximate at the steady state. Meanwhile, the gas temperature was low in the entire cavity.

(b) Fire on the 4th floor:

Within the cavity, smoke moved upwards adhering to the upper inner pane. Meanwhile, the temperature next to the inner pane decreased with an increase in the smoke movement distance. At the higher position in the cavity, smoke was closer to the outer pane.

(c) Fire on the 6th floor:

In the process of spreading upwards within the cavity, smoke adhered to the upper inner pane more markedly and the temperature next to the inner pane was higher than the case when the fire was located on the 4th floor.

It also could be shown in Figure 7 that the temperature at the bottom of the fire room decreased with an increase in the elevation of the fire room.

The above results show that, there were two markedly different scenarios for smoke spread in the cavity as follows.

(1) Scenario 1:

The hot smoke, which was ejected from the fire room, mixed with the cold air from the bottom opening of the cavity, and then spread upwards filling the upper cavity. Consequently, smoke acted at the upper inner and outer glass panes simultaneously with the approximately equal amount of heat. Due to a lot of cold air entraining into the hot smoke, the gas temperature in the cavity was low. When the fire was located on the 2nd floor, the smoke movement in the cavity conformed to scenario 1.

(2) Scenario 2:

At the steady state, smoke moved upwards adhering to the upper inner pane in the cavity. Consequently, the upper inner glass pane might be cracked or even broken in exposing to the hot gases directly. Smoke might then spread to the other floors. When the fire was located on the 4th or 6th floor, the smoke movement in the cavity conformed to scenario 2.

Chow and Hung (2006) had proposed the possibility of these two scenarios in a DSF system, and the different temperature distributions in the cavity could be found from the numerical simulation results by Chow (2011). However, both of them did not further explain the cause resulting in the two scenarios.

Figure 8 presented the velocity distribution at the steady state with Q = 5 MW.

The velocity of cold air flowing into the cavity from the bottom opening was named as V_{air}. According to Figure 8, it could be found that V_{air} had a significant effect on smoke spread in the cavity. The value of V_{air} increased markedly with a decrease in fire room height owing to the influence of stack effect (Yang *et al.* 2013; Shi *et al.* 2014). When the fire source was located on the 2nd floor, the moving path of smoke in the cavity was longer, and stack effect was stronger. Due to the huge suction force of stack effect, V_{air} for the fire on the 2nd floor was higher than the other cases, resulting in a stronger turbulent flow in the cavity. Consequently, the cold air sucked by stack effect mixed with original hot smoke in the cavity. By contrast, stack effect was inconspicuous in the other cases with the fires on the 4th and 6th floors, especially on the 6th floor. Due to the decrease of suction force caused by stack effect, there was less turbulent effect on the hot

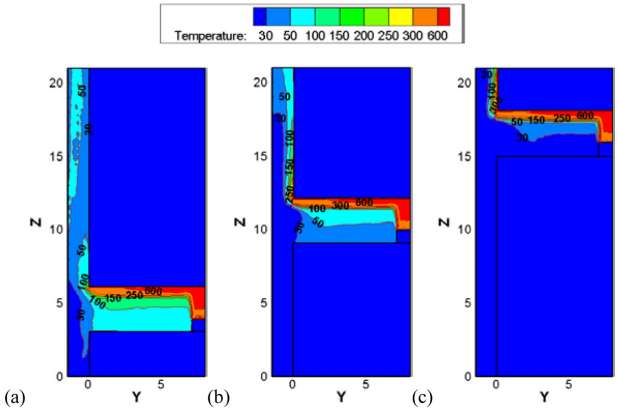

Fig. 7. Temperature distribution at the steady state with Q = 5MW when: (a) Fire on the 2nd floor; (b) Fire on the 4th floor; and (c) Fire on the 6th floor

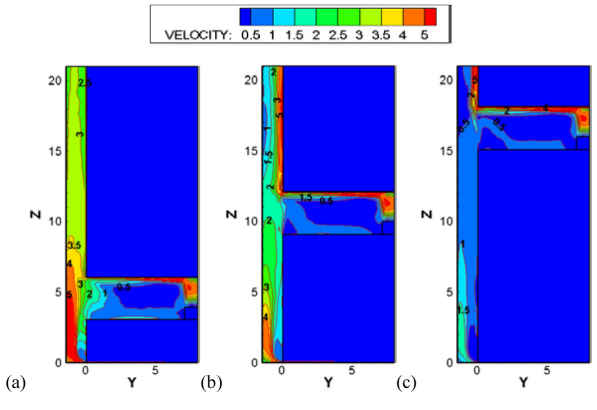

Fig. 8. Velocity distributionat the steady state with Q = 5MW when: (a) Fire on the 2nd floor; (b) Fire on the 4th floor; and (c) Fire on the 6th floor

smoke movement. Therefore, the hot smoke moved upwards more smoothly and adhered to the inner pane by the common function of thermal buoyancy and boundary layer attachment. The boundary layer attachment had also been discovered by Ji *et al.* (2014) on discussing the smoke moving in the shaft on the tunnel ceiling. When a smooth fluid flowed across a convex surface, there was an adsorption tendency to the surface, namely the boundary layer attachment or the Coanda effect. When the smoke moved upwards in the cavity with the smaller effect of airflow from the bottom opening, the smoke moved smoothly, resulting in smoke attachment onto the inner pane.

In conclusion, the stack effect magnitude caused the difference between scenario 1 and scenario 2.

When the cavity depth d varied at 0.8 m, 1.4 m and 2.0 m, the curves of temperature difference between the TI and TO were plotted in Figure 9. The temperature difference TI-TO in different cases shared a similar trend, and the value of TI-TO increased slightly with an increase in cavity depth d , which indicated that the cavity depth was not a key factor determining the smoke spread in the cavity.

4.2. Effects of outer pane tilt angle

When the outer pane tilt angle varied at 80°, 90° and 100°, the vertical temperature profiles next to the inner and outer panes at the steady state were plotted in Figure 10, and Figure 11 presented the corresponding temperature distribution in the DSF system with a 5 MW fire. In view of the vertical temperature profiles with Q = 1 MW shown in Figure 10(a), it was observed that the vertical temperature next to the outer pane (TO) was approximately equal to the environment temperature when θ = 90°. However, its vertical temperature next to the inner pane (TI) was far higher than the environment temperature and gradually reduced with the spread of smoke. For θ = 80°, TI above the fire room was slightly higher than that for θ = 90°. While, TO increased quickly at higher positions, due to the close distance between inner and outer panes near the top of the air cavity with θ = 80°. When increasing fire HRR to 5MW as shown in Figure 10(b), TI was very high and almost equal at the steady state for the outer pane tilt angles of 80° and 90°. In conclusion, for the cases with θ = 80° and θ = 90°, the hot smoke spread upwards in the air cavity adhering to the inner pane, as shown in Figure 11(a) and (b). In these cases, the inner glass pane above the fire room might be cracked or even broken in exposing to the hot gases, resulting in endangering the safety of the other floors above the fire room. When the outer pane gradient was 100° with Q = 1 MW as shown in Figure 10(a), there were slight differences between TI and TO on the upper floors. In addition, the average temperature

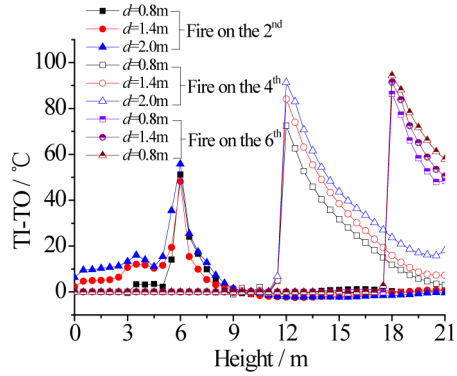

(a) Q = 1MW

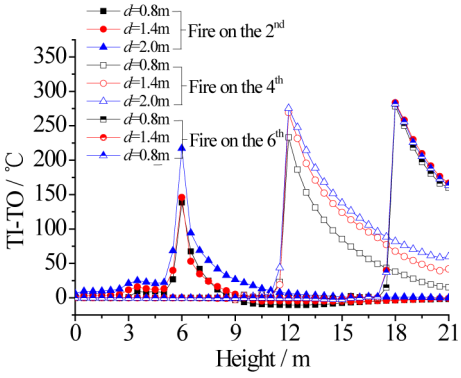

(b) Q = 5 MW

Fig. 9. Curves of TI-TO with the cavity depths of 0.8 m, 1.4 m and 2.0 m

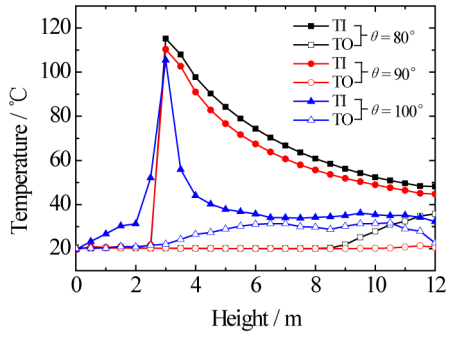

(a) Q = 1MW

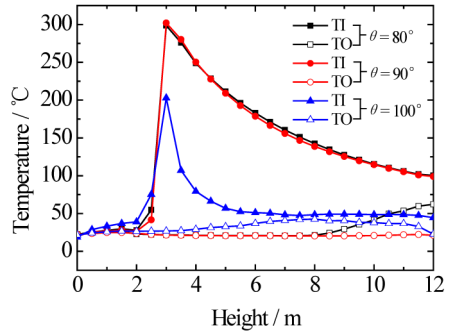

(b) Q = 5MW

Fig. 10. Vertical temperature at the steady state next to the inner and outer panes with the outer pane tilt angle of 80°, 90° and 100°

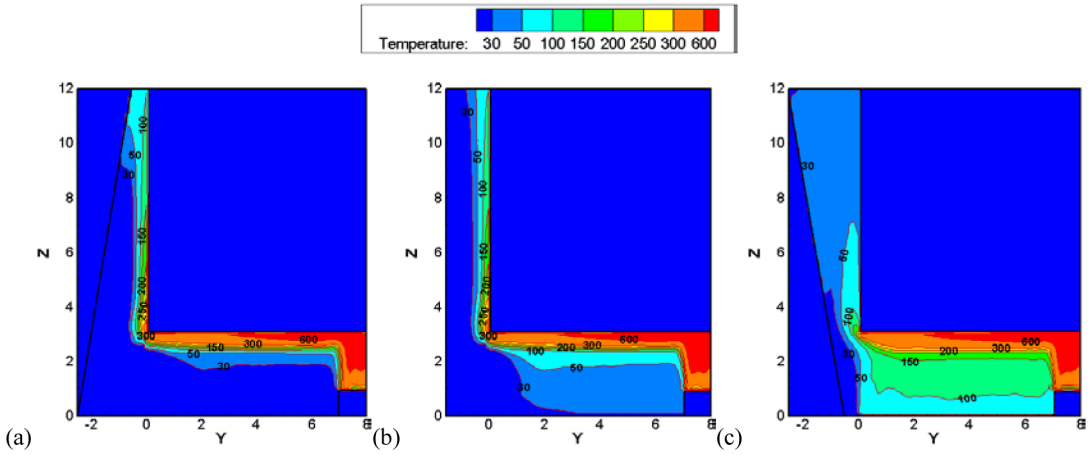

Fig. 11. Temperature distributionat the steady state with Q = 5MW when (a) θ = 80°, (b) θ = 90° and (c) θ = 100°

of TI above the fire room was not higher than 40 °C, which was far lower than the two cases with θ = 80° and θ = 90°. When increasing fire HRR to 5 MW as shown in Figure 10(b), the average temperature of TI was approximately 50 °C. Through observing the temperature distribution in Figure 11(c), the temperature within the cavity was close to be a uniform distribution when θ was 100°. Consequently, it could be inferred that the hot smoke filled the entire cavity between inner and outer panes during spreading upwards, and smoke temperature in the cavity was low.

For further discussing the reason resulting in the different phenomena in those cases, Figure 12 and Figure 13 presented the velocity distribution and the velocity vector diagram at the steady state for Q = 5 MW.

For the outer pane tilt angle of 80° and 90°, gases within the cavity presented laminar motion and flowed smoothly. Meanwhile, the velocity in the vertical flow field varied inversely with its distance from the inner pane. In consideration of temperature distribution as shown in Figure 11(a) and (b), the hot smoke which was ejected out of the fire room spread upwards at a higher speed and there was an adsorption tendency to the inner pane. This was caused by the common function of thermal buoyancy and boundary layer attachment. In many cases, when the smoke moved vertically, it continuously entrains the air. However, the outer pane in the DSF system restrained the entrainment, resulting in attachment onto the inner pane.

For the outer pane tilt angle of 100°, according to the vector flow field within the cavity as shown in Figure 13(c), the smoke moved upward near the side of the inner pane, while the air flowed downwards near the side of the outer pane, resulting in a backflow near the top opening. The reason is that the cavity was a gradually expansion channel from the bottom. According to continuity equation of low speed fluid and Bernoulli equation, the gas velocity decreased and static pressure increased with the expansion of the channel. Therefore, when the smoke flowed along the expansion direction, there would be an adverse pressure gradient in the opposite direction of the smoke movement direction. If the expansion is too fast, the separation phenomenon will occur in the air flow. By the influence of the adverse pressure gradient, the cold

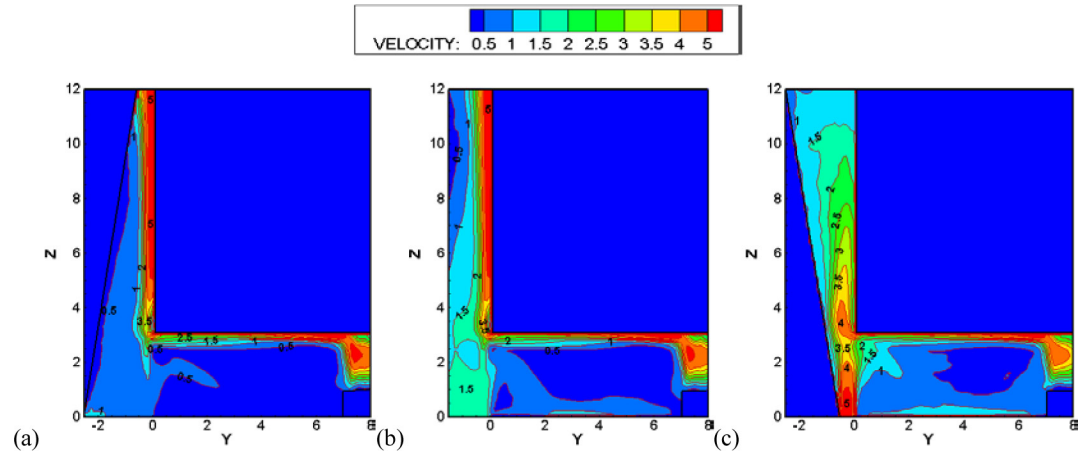

Fig. 12. Velocity distribution at the steady state with Q = 5MW when (a) θ = 80°, (b) θ = 90° and (c) θ = 100°

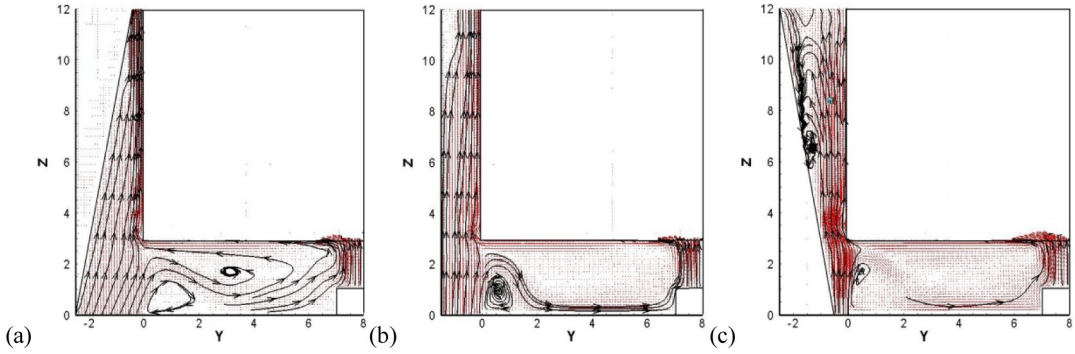

Fig. 13. Velocity vector diagram at the steady state with Q = 5MW when: (a) θ = 80°, (b) θ = 90° and (c) θ = 100°

air flowed into the cavity from the top opening, meanwhile hot smoke moved out of the cavity. The reverse flow of the hot smoke and the cold air produced a turbulent vortex, resulting in mixing with each other. Due to the turbulent vortex, there were several significant effects: on the one hand, it blocked the smoke from moving out of the cavity; on the other hand, the hot smoke mixed with the cold air, which increased the quantity of smoke and decreased the temperature within the cavity.

At the steady state, Figure 14 presented the curves that the smoke layer height in the fire room varied with the distance from the fire in the y direction. It could be found that the outer pane tilt angles influenced markedly on the smoke layer height in the fire room. When Q was 1 MW, the average smoke layer height was 2.41 m for θ = 80°, 2.18 m for θ = 90°, and 1.29 m for θ = 100°.

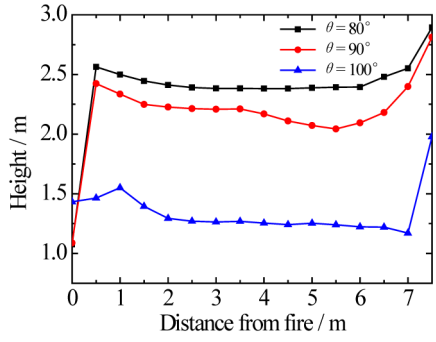

(a) Q = 1MW

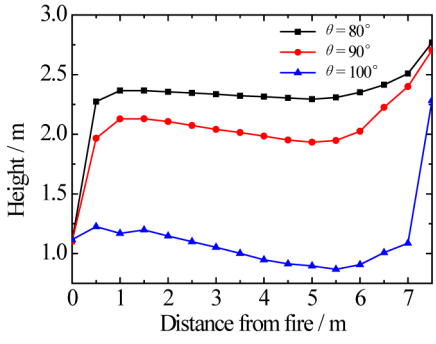

(b) Q = 5MW

Fig. 14. Smoke layer height in the fire room varied with the distance from the fire in the y direction

When Q was 5 MW, the average smoke layer height could decrease to 2.34 m for θ = 80°, 2.05 m for θ = 90°, and 1.02 m for θ = 100°. With the increase in the outer pane tilt angle, the smoke layer thickness in the fire room increased. This tendency was more obvious in the case with θ = 100°. This was because the turbulent vortex blocked the smoke from moving out of the cavity and more hot smoke was accumulated in the fire room.

Conclusions

With various fire room heights and outer pane tilt angles, the smoke spread in the air cavity of a DSF has been studied by CFD in this paper. All simulations were under two HRRs of 1 MW and 5 MW. The results are summarized as follows:

With the fire room located adjacent to the DSF on the 2nd, 4th and 6th floors, 18 cases were designed to discuss the effects of fire room height. Results suggested that two scenarios of smoke movement might occur in the cavity. When a fire erupted on a lower floor, it conformed to scenario 1. Due to the stronger chimney effect, smoke filled the upper cavity and acted at the upper inner and outer glass panes simultaneously with the approximately equal amount of heat. However, when a fire erupted on a higher floor, it conformed to scenario 2. In this scenario, the hot smoke moved upwards in the cavity adhering to the upper inner pane. It was dangerous for the upper floors as the upper inner glass pane might be cracked or even broken in exposing to the hot gases directly.

The outer pane tilt angles of 80°, 90° and 100° were considered in this paper with 6 cases. The simulation results suggested that the hot smoke moved upwards at a higher speed and adhered to the inner pane in the cavity of a DSF with an inward tilted or vertical outer pane. Therefore, the inner glass pane above the fire room might be cracked or even broken in exposing to the hot gases. However, when the smoke moved upwards in the cavity of a DSF with an outward tilted outer pane, there was a turbulent vortex due to the influence of the adverse pressure gradient. The turbulent vortex prevented hot smoke flowing out of the fire room but decreased the temperature within the cavity.

In a word, this study attempts to enhance the understanding of how smoke spread within a cavity of a DSF. Results suggested that the higher fire room and the inward tilted or vertical outer pane will be dangerous for the upper inner glass pane and rooms. Our findings could be beneficial for engineers to design fire protection codes in buildings.

Acknowledgement

This work was supported by National Natural Science Foundation of China (NSFC) under Grant No. 51376173 and the National Basic Research Program of China (973 Program) under Grant No. 2012CB719700.

References

Chan, A. L. S.; Chow, T. T.; Fong, K. F.; Lin, Z. 2009. Investigation on energy performance of double skin façade in Hong Kong, *Energy and Buildings* 41(11): 1135–1142. http://dx.doi.org/10.1016/j.enbuild.2009.05.012

Chen, J. L. 2010. A discussion on the fire characteristics and countermeasures of curtain wall, *Jiangxi Chemical Industry* 3: 137–138.

Chow, C. L. 2011. Numerical studies on smoke spread in the cavity of a double-skin façade, *Journal of Civil Engineering and Management* 17(3): 371–392. http://dx.doi.org/10.3846/13923730.2011.595075

Chow, C. L.; Chow, W. K. 2009. Fire safety aspects of refuge floors in supertall buildings with computational fluid dynamics, *Journal of Civil Engineering and Management* 15(3): 225–236. http://dx.doi.org/10.3846/1392-3730.2009.15.225-236

Chow, W. K. 1996. Application of computational fluid dynamics in building services engineering, *Building and Environment* 31(5): 425–436. http://dx.doi.org/10.1016/0360-1323(96)00012-1

Chow, W. K.; Hung, W. Y. 2006. Effect of cavity depth on smoke spreading of double-skin façade, *Building and Environment* 41(7): 970–979. http://dx.doi.org/10.1016/j.buildenv.2005.04.009

Chow, W. K.; Hung, W. Y.; Gao, Y.; Zou, G.; Dong, H. 2007. Experimental study on smoke movement leading to glass damages in double-skinned façade, *Construction and Building Materials* 21(3): 556–566. http://dx.doi.org/10.1016/j.conbuildmat.2005.09.005

Ding, W. T.; Hasemi, Y. 2006. Smoke control through a double-skin façade used for natural ventilation, *ASHRAE Transactions* 112(Pt 1): 181–188.

Ding, W. T.; Hasemi, Y. J.; Yamada, T. 2005. Natural ventilation performance of a double-skin façade with a solar chimney, *Energy and Buildings* 37(4): 411–418. http://dx.doi.org/10.1016/j.enbuild.2004.08.002

Gratia, E.; De Herde, A. 2004a. Natural cooling strategies efficiency in an office building with a double-skin façade, *Energy and Buildings* 36(11): 1139–1152. http://dx.doi.org/10.1016/j.enbuild.2004.05.004

Gratia, E.; De Herde, A. 2004b. Natural ventilation in a double-skin façade, *Energy and Buildings* 36(2): 137–146. http://dx.doi.org/10.1016/j.enbuild.2003.10.008

Gratia, E.; De Herde, A. 2004c. Optimal operation of a south double-skin façade, *Energy and Buildings* 36(1): 41–60. http://dx.doi.org/10.1016/j.enbuild.2003.06.001

Gratia, E.; De Herde, A. 2007a. Guidelines for improving natural daytime ventilation in an office building with a double-skin façade, *Solar Energy* 81(4): 435–488. http://dx.doi.org/10.1016/j.solener.2006.08.006

Gratia, E.; De Herde, A. 2007b. Are energy consumptions decreased with the addition of a double-skin?, *Energy and Buildings* 39(5): 605–619. http://dx.doi.org/10.1016/j.enbuild.2006.10.002

Guo, D. G.; He, W.; Xu, W. X. 2004. Performance-based fire safety analysis for a double skin façade, *Fire Science and Technology* 23(4): 341–344.

Guo, S. D.; Yang, R.; Zhang, H.; Narayanan, S.; Atalla, M. 2009. Development of a fire zone model considering mixing behavior, *Journal of Thermophysics and Heat Transfer* 23(2): 327–338. http://dx.doi.org/10.2514/1.41240

He, Z. H.; Mu, Y. J. 2003. The computational fluid dynamics analysis on the fire characteristics of double-skin façade, *Zhejiang Fire* 7: 40–42.

Hien, W. N.; Wang, L. P.; Chandra, A. N.; Pandey, A. R.; Wei, X. L. 2005. Effects of double glazed facade on energy consumption, thermal comfort and condensation for a typical office building in Singapore, *Energy and Buildings* 37(6): 563–572. http://dx.doi.org/10.1016/j.enbuild.2004.08.004

Ji, J.; Fan, C. G.; Gao, Z. H.; Sun, J. H. 2014. Effects of vertical shaft geometry on natural ventilation in urban road tunnel fires, *Journal of Civil Engineering and Management* 20(4): 466–476. http://dx.doi.org/10.3846/13923730.2013.801916

Kim, S. Y.; Song, K. D. 2007. Determining photosensor conditions of a daylight dimming control system using different double-skin envelope configurations, *Indoor and Built Environment* 16(5): 411–425. http://dx.doi.org/10.1177/1420326X07082497

McGrattan, K.; Hostikka, S.; Floyd, J.; Klein, B.; Prasad, K. 2009a. *Fire dynamics simulator* (Version 5). Technical Reference Guide. National Institute of Standards and Technology Special Publication 1018-5.

McGrattan, K. B.; Klein, B.; Hostikka, S.; Floyd, J. E. 2009b. *Fire dynamics simulator* (Version 5). User's guide. National Institute of Standards and Technology Special Publication 1019-5. 186 p.

Ni, Z. P.; Lu, S. C.; Zhi H. Q.; Wang, L. 2007. Full scale fire case on the double skin façade, *Fire Safety Science* 16(4): 232–242.

Ni, Z. P.; Zhi, H. Q.; Lu, S. C.; Wang, L. 2008. Numerical simulation on the study of the fire properties of double curtain wall, *Journal of Safety and Environment* 8(2): 129–134.

Shi, W. X.; Ji, J.; Sun, J. H.; Lo, S. M.; Li, L. J.; Yun, X. Y. 2014. Experimental study on influence of stack effect on fire in the compartment adjacent to stairwell of high rise building, *Journal of Civil Engineering and Management* 20(1): 121–131. http://dx.doi.org/10.3846/13923730.2013.802729

Smagorinsky, J. 1963. General circulation experiments with the primitive equations, *Monthly Weather Review* 91(3): 99–164. http://dx.doi.org/10.1175/1520-0493

Wang, J.; Wu, Z. K.; Xiao, X. F.; He, Y. P. 2005. Determination of fire scenario in performance-based fire safety design, *Fire Science and Technology* 24(3): 274–278.

Wigginton, M. 1996. *Glass in architecture*. 1st ed. London: Phaidon. 320 p.

Yang, D.; Du, T.; Peng, S. N.; Li, B. Z. 2013. A model for analysis of convection induced by stack effect in a shaft with warm airflow expelled from adjacent space, *Energy and Buildings* 62: 107–115. http://dx.doi.org/10.1016/j.enbuild.2013.02.045

Zhang, X. C.; Yang, M. J.; Wang, J. A.; He, Y. P. 2010. Effects of computational domain on numerical simulation of building fires, *Journal of Fire Protection Engineering* 20(4): 225–251. http://dx.doi.org/10.1177/1042391510367349

Zhu, S.; Huo, R.; Hu L. H.; Yang, D. 2008. Influence of mesh grid and computational domain on FDS simulation, *Journal of Safety and Environment* 8(4): 131–134.

Jie JI. He is an Associate Professor of State Key Laboratory of Fire Science, University of Science and Technology of China, and is also a life member of International Association of Fire Safety Science. He received his PhD degree in Fire Safety Engineering from University of Science and Technology of China in 2008. His main research interests include smoke movement and ventilation control method in tunnel and building fires.

Yi Fan LI. She is a Postgraduate of University of Science and Technology of China from September 2010 to present. Her research interest includes smoke spread and control method in high rise buildings.

Wen Xi SHI. He is a Doctoral Student of University of Science and Technology of China from September 2011 to present, and he has participated in joint training project of the University of Science and Technology of China and City University of Hong Kong in 2010. His research interest includes smoke spread and control method in high rise buildings.

Jin Hua SUN. He is a Professor and Vice Director of State Key Laboratory of Fire Science, University of Science and Technology of China. He is also a Vice Chairman of Asia-Oceania Association for Fire Science and Technology and director of the International Association for Fire Safety Science. He received his PhD from the University of Tokyo in 1999. To date he has authored over 200 research papers of which 100 were indexed by SCI and EI, including over 20 published in h-factor top journals and six books. His main research interests include fire dynamics and basic fire prevention technologies, large-scale evacuation and rescue in emergencies, hazardous chemical disaster prediction and prevention methods.